Notes on Reproducibility of $Ge_2Sb_2Te_5$ Properties

Keiji Tanaka

Sputtered $Ge_2Sb_2Te_5$ films have been utilized in phase-change devices, while quantitative reproducibility of fundamental properties such as refractive index and electrical conductivity remains unsatisfactory. The present work exemplifies that the properties are considerably affected by sputter conditions. It seems that high-quality amorphous films can be deposited with slow dc sputtering under high voltages and low Ar pressures. We also discuss whether the cubic $Ge_2Sb_2Te_5$ is a degenerate or a non-degenerate semiconductor.

Keywords
amorphous, chalcogenide, phase-change, sputter, electrical conductivity

Conflict of Interest
The author declares no conflict of interest.

Prof. Em. K. Tanaka
Department of Applied Physics, Graduate School of Engineering, Hokkaido University, Kita-ku, 060-8628 Sapporo, Japan
E-mail: keiji@eng.hokudai.ac.jp

1. Introduction

$Ge_2Sb_2Te_5$ films have been commercialized in optical phase-change disks and electrical memories,[1,2] and are currently being developed to innovative devices including neuromorphic circuits[3,4] and integrated photonic memories.[2,5] These new applications employ multi-level operations with subtle optical or electrical changes,[2-5] while what is surprising is that related fundamental properties have scarcely been reproduced. For instance, in contrast to more-or-less fixed optical-gap energies of 0.7 – 0.9 eV in the amorphous films,[6-11] refractive indices reported so far scatter over 3.3 – 4.5 (at $\lambda \approx 1 -$ 2 μm)[1,2,8,9,11-15] and electrical conductivities at room temperatures extend over two orders of magnitude (see, **Figure 2**).

Why is the data reproducibility so poor? Here, we may notice that one of the reasons is due to undetailed descriptions of sputtering conditions of inspected films in previous works, except a few.[8,13,16,17] Besides, in many studies, film compositions are approximated at $Ge_2Sb_2Te_5$ (abbreviated as GST hereafter), with accurate atomic compositions being not specified. It is plausible that such circumstances give rise to different features not only in the amorphous but also in the corresponding crystalline films. The present work discusses some factors causing non-reproducible results, which will be valuable to further advancement of the phase-change devices. Discussion will be given also on electrical properties of meta-stable, cubic GST films.

2. Sputtering conditions

Since the amorphous state is quasi-stable, it is natural that all the properties of amorphous (a-) GST films depend upon preparation details. For instance, the author's group employed a small dc magnetron sputtering system,[7,18,19] in which important parameters were applied voltage V (≤ 5 kV for a target-substrate distance of 1.5 cm) and plasma current I_p (≤ 2 mA for a $Ge_{12}Sb_{25}Te_{63}$ target with a diameter of 5 cm); the latter could be adjusted by Ar-gas (99.9995% purity) pressure. Substrate temperature was not controlled, and it might rise to ~50°C during sputtering. And, preliminary experiments demonstrated that the sputtering rate increased in proportion to $(V - V_t)I_p$, where $V_t \approx 0.5$ kV, and it was maximal at ~25 nm/min under 2.5 kV and 2 mA. Above 2.5 kV, spontaneous sparks could not be suppressed, despite of a power supply equipping a spike filter.

Table 1 summarizes some properties of deposited a-GST films as a function of the sputtering voltage at $I_p = 0.5$ mA Note that electron-microprobe analyses with an accuracy of ±1 at.% demonstrated the precise composition of the films to be $Ge_{22}Sb_{24}Te_{54}$, which was independent of the applied voltage. We see that sputtering at higher voltages produces films with wider optical gaps (an example being shown in Ref. 7), higher refractive indices, and smoother surfaces. As mentioned later, the higher index can be related with a higher film density through the Lorentz-Lorenz law,* which implies that higher-voltage sputtering can

Table 1. Variations of sputtering conditions and physical properties of deposited a-GST as a function of the sputtering voltage (1 – 2.5 kV) under a fixed plasma current of 0.5 mA; Tauc optical gap energy E_g, refractive index n at $\lambda \approx 2$ μm, thermal activation energy E_a of the electrical conductivity, root-mean-square surface roughness, and the fractional thickness reduction (from amorphous to cubic phases) d_c/d_a with annealing at ~250°C for ~30 min, where $d \approx 500$ nm. The optical gap was calculated from transmission spectra, the refractive index was evaluated from optical interference fringes, and the film thickness and the roughness were probed using an atomic force microscope equipping cantilevers with an apex curvature of ~10 nm.

Voltage	Ar pressure	Sputtering rate	E_g	n	E_a	Roughness	d_c/d_a
1.0 kV	1.0 mTorr	0.5 nm/min	0.70 eV	3.6	0.37 eV	5 nm	85%
1.5	0.70	3.2	0.72	4.5	0.45	3	90
2.0	0.55	5.0	0.74	4.5	0.46	3	93
2.5	0.45	5.2	0.74	4.5	0.45	2	95

produce more dense films. On the other hand, with an increase in the sputtering current, the film surface tended to become rough. For instance, as shown in **Figure 1**, under variation of I_p = 0.5 – 2 mA at V = 2.5 kV, the roughness increased by three times, with the averaged particle size appearing to be constant at 50 ± 20 nm.

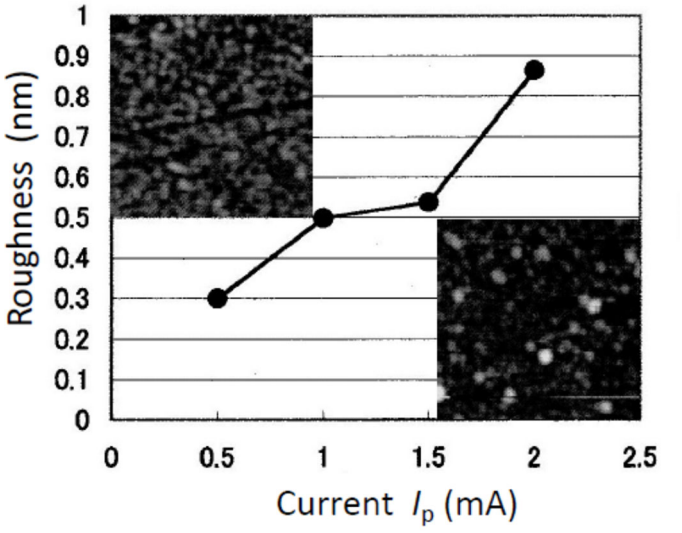

Figure 1. Root-mean-square surface roughness of GST films with thicknesses of 60 ± 10 nm as a function of the plasma current I_p at V = 2.5 kV. The upper-left and the lower-right photographs exemplified the surfaces (side lengths of 500 nm) at I_p = 0.5 and 2 mA with black-white amplitudes of 3 and 6 nm, respectively.

[footnote] *It is not straightforward to evaluate the density of thin films,[13,20] and instead the refractive index seems to be a good measure of structural compactness.

Taking these observations into account, Kato and Tanaka[7] adopted the sputtering condition of 2.5 kV and 0.5 mA, which gave rise to a slow deposition rate of ~5 nm/min. Note that this current was obtained at an Ar pressure of ~0.5 mTorr (≈ 70 mPa), which is appreciably lower than those commonly employed, 1 – 15 mTorr.[2,8,13,15,16,21] It was also noticed that, in the films thinner than ~10 nm, data reproducibility was worse and the crystallization (to the cubic phase) at ~160°C became vaguer, in consistent with previous observations,[2,21] which are probably due to substrate contamination, island thin-film structures

and/or surface oxidation.

Here, a remark on the correlation between the refractive index n and the thickness ratio d_c/d_a in **Table 1** may be in order. It has been demonstrated that the cubic crystal, which is a meta-stable phase, can be obtained through annealing of amorphous films at temperatures of ~200°C, above the crystallization temperature of ~160°C. (Or, the crystalline film can directly be deposited onto heated substrates.) As shown in **Table 1**, the annealing also made the amorphous films, which were sputtered at 1.0 – 2.5 kV, thinner by 85 – 95%, the result being similar to that reported by Kim et al.[16] Provided that the produced crystalline films have a fixed density, this fact implies that the amorphous film deposited at 2.5 kV is the most dense, which is consistent with its maximal refractive index. Actually, the Lorentz-Lorenz law can provide a quantitative correlation between n and d_c/d_a, which enforces the idea. Incidentally, the film thicknesses after annealing treatments at 200 and 300°C appeared within sample-to-sample variations of a few percent, which is consistent with the fact that the densities of the cubic and hexagonal phases are nearly the same.[23]

3. Electrical conductivity

Figure 2 summarizes electrical conductivities σ of GST.[6,7,17,23-33] The conductivity in the amorphous films at room temperature distributes over 10^{-4} – 10^{-2} S/cm, in which the present film[7] is located at a lower part of reported data. On the other hand, the thermal activation energy E_a is calculated to be ~0.45 eV (**Table 1**), which is comparable with previous values.[23,24,26-28,31,33] Here, it may be worth mentioning that no difference in the electrical conductivity was discernible for samples attached with coplanar and sandwich electrodes of deposited Au or Pt films.

Figure 2 also includes the conductivity of the cubic phase obtained through annealing treatments.[6,7,17,27] Surprisingly, published data are relatively a few, despite of important roles of the phase in electrical devices. The conductivities at room temperature scatter over 10^0 – 10^2 S/cm, in which the present films appear to be less conductive, 10^0 – 10^1 S/cm; the value being substantially affected by the annealing temperatures of 200 and 250°C. A similar variation has also been reported by Burr et al.[17]

How can we grasp such scattered conductivities of the cubic phase? At the outset, it may be reasonable to assume that the annealing temperature governs film structures leading to different conductivities. However, x-ray patterns of the present films,[7] exemplified in **Figure 3**, substantiated that the crystallite size evaluated by applying the Scherrer's equation to the 200 peak (at $2\theta \approx 30°$) was ~15 nm, irrespective of the annealing temperatures of 200 and 250°C (with a heating rate of 5 − 10°C/min and a holding duration of 10 min in Ar atmosphere); the behaviour being similar to that reported in Refs. 2 and 11. Nevertheless, since the amorphous structure provides broad low-intensity halos, it is plausible that non-crystalline regions and/or e

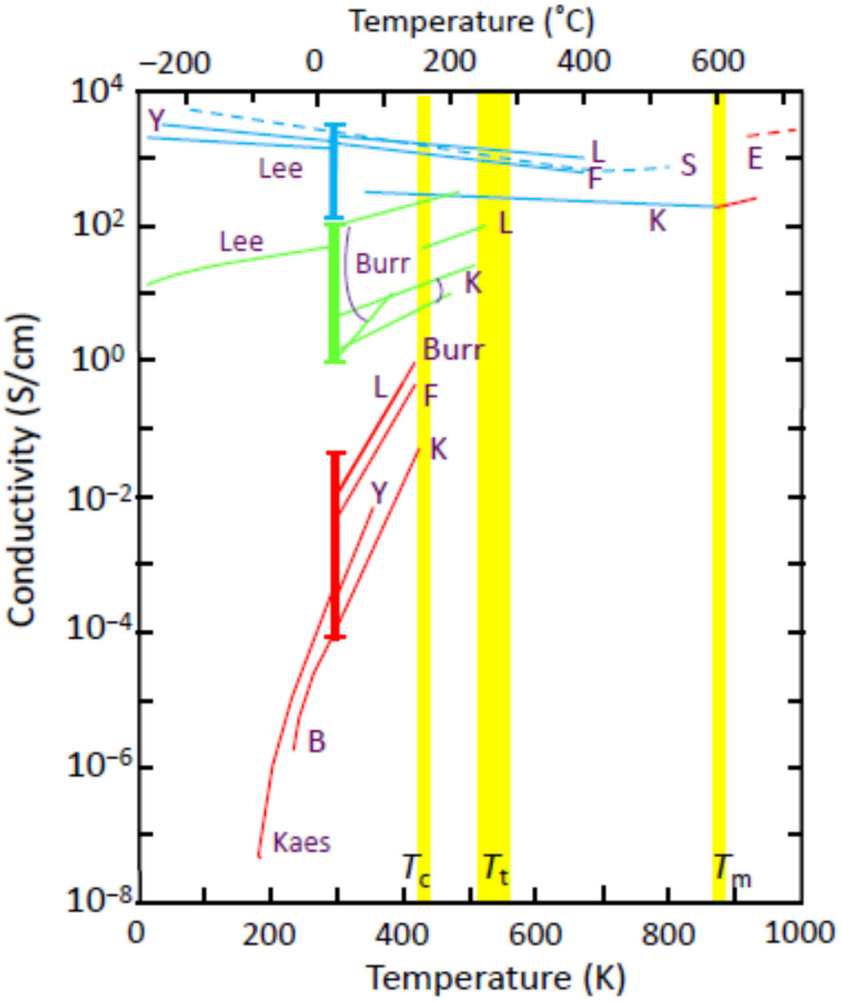

Figure 2. Temperature variations of electrical conductivities in amorphous (red), cubic (green), hexagonal (blue) and liquid (red) GST; B for Baily et al.,[28] Burr et al.,[17] E for Endo et al.,[30] F for Friedrich et al.,[24] Kaes et al.,[31] K for Kato and Tanaka,[7] L for Lankhorst et al.,[27] Lee et al.,[6] S for Shelimova et al.,[25] Y for Yamanaka et al.[26] Burr and L for amorphous films mostly overlap. Solid and dashed lines in the hexagonal[6,7,24-27] and liquid[7,30] phases are obtained, respectively, for films and for bulk samples. The two lines for the cubic films, Burr and K, are obtained upon cooling processes after annealing at different temperatures (140 – 250°C). Three error bars represent data scattering in amorphous, cubic and hexagonal films at room temperature,[15,22,29,31-33] and three yellow bands show the crystallization (T_c), transformation (T_t), and melting (T_m) temperatures.[1,2]

grain boundaries still remain,[17] which affect the scattered conductivities.

The assertion that the hexagonal phase is a degenerate semiconductor with negative temperature coefficients, $\partial\sigma/\partial T < 0$, has been documented in all the studies shown in **Figure 2**.[6,7,24-27] However, the figure also manifests that the conductivities at room temperature scatter by an order, in which the present film is less conductive than those of bulk samples,[22,25] which may reflect different grain sizes. Incidentally, the x-ray evaluated crystallite size of the present films annealed at ~300°C (**Figure 3**) was 50 – 100 nm.

Finally, **Figure 2** also reveals that the conductivity above the melting temperature of ~600°C[1,2] of the hexagonal phase is thermally activated with $E_a \approx 0.2$ eV.[7,30] Interestingly, the disordered phases, both liquid and amorphous, appear to be semiconductors. Here, it seems reasonable that the conductivity obtained

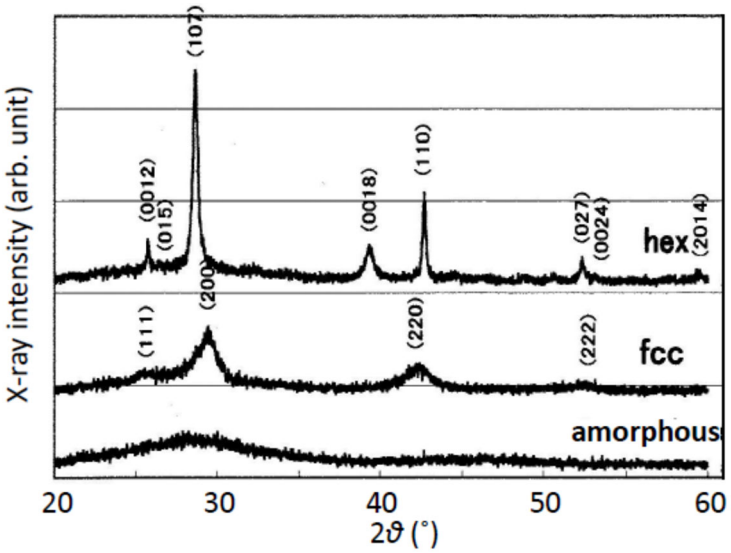

Figure 3. X-ray diffraction patterns of amorphous (as-sputtered), cubic, and hexagonal GST films ($d \approx 500$ nm), taken using a grazing-incident Cu K_α beam emitted from a rotating anode. The cubic and hexagonal phases are obtained by annealing at 185 and 300°C, respectively, for 10 min in Ar-gas atmosphere. The peak indices follow previous studies.[2,9,11,24]

using SiO_2-coated GST films in Ref. 7 is lower than that in bulk samples,[30] due to surface effects and so forth.

4. Electrical conductivity in cubic $Ge_2Sb_2Te_5$

An interesting problem is what governs the dramatic changes in the conductivity σ between amorphous, cubic, and hexagonal phases. Simply, $\sigma = eN\mu$ for a unipolar system, where N is the carrier (hole) [6,7] density and μ the (drift) mobility, and we wonder which factor is more responsible for the conductivity changes. With this regard, characterization of the cubic phase appears to be crucial, for which two ideas have been presented. Lee et al.[6] demonstrated using Hall measurements that $N \approx 10^{20}$ cm^{-3} even at 5 K, asserting that the cubic phase (and also the hexagonal phase) is a *degenerate* semiconductor. They also assume that the σ change at the amorphous-to-cubic transformation is governed by N changes, reflecting shifts of the Fermi level, which originate from some bond exchanges in short-range structures; the idea being followed by other researchers.[2,34] By contrast, Kato and Tanaka[7] proposed through conductivity and thermo-power measurements that $\mu \approx 10^{-2} - 10^{-3}$ cm^2/(Vs) in a-GST, in consistent with Xus' results,[10] and the σ increase at the amorphous-to-cubic transformation is governed by dramatic mobility enhancements to ~10^2 cm^2/(Vs) with mostly fixed N of ~10^{16} cm^{-3}. (And the cubic-to-hexagonal is by an increase in N to ~10^{20} cm^{-3} with $\mu \approx 10 - 10^2$ cm^2/(Vs).[7,22,25]) In short, both models presume that the cubic GST is a hole-conductive semiconductor, while it may be degenerate[6] or nearly *intrinsic*.[7] How can we compromise these ideas? Here, we should take at least two facts into account.

One is that the present GST film is slightly Sb-rich, with a composition of $Ge_{22}Sb_{24}Te_{54}$. And, Yamada and Matsunaga[35] have suggested that, when Sb-rich amorphous films are laser-crystallized, those form two-phase structures consisting of cubic $Ge_2Sb_2Te_5$ and amorphous Sb regions. Provided that such a model could be applied to the annealed film, as in the present case, it is nonetheless difficult to predict what governs the electrical property in heterogeneous

films; e.g., not only the two fractions but also percolative structures would affect the conductivity. More generally, although the compositional deviation from stoichiometry might be neglected in amorphous states, due to reduced electronic states by flexible atomic connectivity, the excess atoms are likely to produce donor or acceptor-like states in the corresponding crystal. Unfortunately, precise composition in Lees' samples has been unspecified,[6] and accordingly, it is difficult to pursue further speculation.

The other is that the preparation procedures of the amorphous films, rf sputtering in Lee et al.[6] and dc sputtering in Kato and Tanaka,[7] could exert substantial influences. These methods produce a-GST films with similar optical absorption-edge spectra,[6,7] while there may be some differences in sub-gap absorptions, the detail of the dc-sputtered films being inspected recently.[36] We have also seen that the dc sputtering under high voltages with slow rates (~5 nm/min) deposits more compact amorphous films, which could favour producing dense cubic films possessing fewer cation (Sb/Ge) vacancies,[37,38] smaller N, and lower σ. In contrast, although no preparation details being given, the Lees' films might be deposited at a faster rate, e.g. ~5 nm/s, in a similar way to that commonly employed,[24] which may contain more vacancies and/or voids, giving rise to smaller refractive index, more dangling bonds and N, and higher σ. It is plausible that such structural differences modify the Fermi-level position also in the crystalized films. Thus, for obtaining reproducible results, it will be valuable to regard the density, or the refractive index in materials having nearly the same optical gap, of amorphous films as an important, macroscopic measure.

5. Conclusions

The present and previous data demonstrate that preparation conditions in sputtering exert strong influences upon physical properties such as the refractive index and electrical conductivity of amorphous and crystalline GST films. Specifically, good-quality amorphous films can be obtained through slow deposition (at low Ar pressure) under a high dc voltage. Besides, the conductivity of cubic GST appears to be critically affected by deposition and annealing procedures.

Acknowledgements

The author would like to thank his former students and colleague, T. Kato, K. Sugawara, H. Satoh and T. Gotoh, who had perseveringly performed fundamental experiments of GST films.

[1] N. Yamada, *Phys. Status Solidi B* **2012,** 249, 1837.
[2] P. Guo, A. M. Sarangan, I. Agha, *Appl. Sci.* **2019,** 9, 530.
[3] S. R. Ovshinsky, *Jpn. J. Appl. Phys.* **2004,** 43, 4695.

[4] G. W. Burr, R. M. Shelby, A. Sebastian, Sa. Kim, Se. Kim, S. Sidler, K. Virwani, M. Ishii, P. Narayanan, A. Fumarola, L. L. Sanches, I. Boybat, M. Le Gallo, K. Moon, J. Woo, H. Hwang, Y. Leblebici, *Adv. Phys.: X* **2017,** 2, 89.

[5] E. Kuramochi, M. Notomi, *Nat. Photonics* **2015,** 9, 712.

[6] B. -S. Lee, J. R. Abelson, S. G. Bishop, D. -H. Kang, B. Cheong, K. -B. Kim, *J. Appl. Phys.* **2005,** 97, 093509.

[7] T. Kato, K. Tanaka, *Jpn. J. Appl. Phys.*, **2005,** 44, 7340.

[8] J. K. Olson, H. Li, T. Ju, J. M. Viner, P. C. Taylor, *J. Appl. Phys.* **2006,** 99, 103508.

[9] J. -W. Park, S. H. Eom, and H. Lee, J. L. F. Da Silva, Y. -S. Kang, T. -Y. Lee, Y. H. Khang, *Phys. Rev. B* **2009,** 80, 115209.

[10] L. Xu, L. Tong, L. Geng, F. Yang, J. Xu, W. Su, D. Liu, Z. Ma, K. Chen, *J. Appl. Phys.* **2011,** 110, 013703.

[11] Z. Xu, C. Chen, Z. Wang, K. Wu, H. Chong, H. Ye, *RSC Adv.* **2018,** 8, 21040.

[12] S. Y. Kim, S. J. Kim, H. Seo, M. R. Kim, *Jpn. J. Appl. Phys.* **1999,** 38, 1713.

[13] H. Dieker, M. Wuttig, *Thin Solid Films* **2005,** 478, 248.

[14] K. Shimakawa, L. Střižik, T. Wagner, M. Frumar, *APL Mater.* **2015,** 3, 041801.

[15] C. Chen, P. Jost, H. Volker, M. Kaminski, M. Wirtssohn, U. Engelmann, K. Krüger, F. Schlich, C. Schlockermann, R. P. S. M. Lobo, M. Wuttig, *Phys. Rev. B* **2017,** 95, 094111.

[16] J. -H. Kim, *J. Appl. Phys.* **1999,** 86, 6770.

[17] G. W. Burr, P. Tchoulfian, T. Topuria, C. Nyffeler, K. Virwani, A. Padilla, R. M. Shelby, M. Eskandari, B. Jackson, B. -S. Lee, *J. Appl. Phys.* **2012,** 111, 104308.

[18] H. Satoh, K. Sugawara, K. Tanaka, *J. Appl. Phys.* **2006,** 99, 024306.

[19] A. Saitoh, T. Donuma, K. Tanaka, *Appl. Phys. Express* **2008,** 1, 021501.

[20] Y. Tatsumi, H. Ohsaki, Y. Kurahashi, M. Iijima, K. Kurumi, K. Miura, T. Ino, *Jpn. J. Appl. Phys.* **1986,** 25, 1152.

[21] H. -Y. Cheng, S. Raoux, Y. -C. Chen, *J. Appl. Phys.* **2010,** 107, 074308.

[22] J. M. Yanez-Limon, J. Gonzalez-Hernandez, J. J. Alvarado-Gil, I. Delgadillo, H. Vargas, *Phys. Rev. B* **1995**, 52, 16321.

[23] W. K. Njoroge, H. -W. Wöltgens, M. Wuttig, *J. Vac. Sci. Technol.* A **2002,** 20, 230.

[24] I. Friedrich, V. Weidenhof, W. Njoroge, P. Franz, M. Wuttig, *J. Appl. Phys.* **2000,** 87, 4130.

[25] L. E. Shelimova, O. G. Karpinskii, P. P. Konstantinov, M. A. Kretova, E. S. Avilov, V. S. Zemskov, *Inorg. Mater.* **2001,** 37, 342.

[26] S. Yamanaka, S. Ogawa, I. Morimoto, Y. Ueshima, *Jpn. J. Appl. Phys.* **1998,** 37, 3327.

[27] M. H. R. Lankhorst, B. W. S. M. M. Ketelaars, R. A. M. Wolters, *Nat. Mater.* **2005,** 4, 347.

[28] S. A. Baily, D. Emin, H. Li, *Solid St. Commun.* **2006,** 139, 161.

[29] M. Boniardi, A. Redaelli, A. Pirovano, I. Tortorelli, D. Ielmini, F. Pellizzer, *J. Appl. Phys.* **2009,** 105, 084506.

[30] R. Endo, S. Maeda, Y. Jinnai, R. Lan, M. Kuwahara, Y. Kobayashi, M. Susa, *Jpn. J. Appl.*

Phys. **2010,** 49, 065802.
[31] M. Kaes, M. L. Gallo , A. Sebastian, M. Salinga, D. Krebs, *J. Appl. Phys.* **2015,** 118, 135707.
[32] N. Saxena, A. Manivannan *J. Phys. D: Appl. Phys.* **2019,** 52, 375301.
[33] J. Rocca, J. L. García, M. A. Ureña, M. Fontana, B. Arcondo, *Mater. Res.* **2019,** 22, e20180512.
[34] J. Robertson, *Phys. Status Solidi A* **2016,** 213, 1641.
[35] N. Yamada, T. Matsunaga, *J. Appl. Phys.* **2000,** 88, 7020.
[36] T. Gotoh, *Phys. Status Solidi B* **2019,** 1900278.
[37] J. Zhou, Z. Sun, Y. Pan, Z. Song, R. Ahuja, *EPL* **2011,** 95, 27002.
[38] F. Yang, T. Chen, M. Wang, B. Yan, L. Wan, D. Ke, Y. Dai, *AIP Adv.* **2018,** 8, 065223.